NREL
NATIONAL RENEWABLE ENERGY LABORATORY

Gearbox Reliability Collaborative High Speed Shaft Tapered Roller Bearing Calibration

J. Keller and Y. Guo
National Renewable Energy Laboratory

B. McNiff
McNiff Light Industry

NREL is a national laboratory of the U.S. Department of Energy
Office of Energy Efficiency & Renewable Energy
Operated by the Alliance for Sustainable Energy, LLC

This report is available at no cost from the National Renewable Energy Laboratory (NREL) at www.nrel.gov/publications.

Technical Report
NREL/TP-5000-60319
October 2013

Contract No. DE-AC36-08GO28308

NREL
NATIONAL RENEWABLE ENERGY LABORATORY

Gearbox Reliability Collaborative High Speed Shaft Tapered Roller Bearing Calibration

J. Keller and Y. Guo
National Renewable Energy Laboratory

B. McNiff
McNiff Light Industry

Prepared under Task No. WE11.0301

National Renewable Energy Laboratory
15013 Denver West Parkway
Golden, CO 80401
303-275-3000 • www.nrel.gov

Technical Report
NREL/TP-5000-60319
October 2013

Contract No. DE-AC36-08GO28308

This report is available at no cost from the National Renewable Energy Laboratory (NREL) at www.nrel.gov/publications.

Available electronically at http://www.osti.gov/bridge

Available for a processing fee to U.S. Department of Energy and its contractors, in paper, from:

U.S. Department of Energy
Office of Scientific and Technical Information
P.O. Box 62
Oak Ridge, TN 37831-0062
phone: 865.576.8401
fax: 865.576.5728
email: mailto:reports@adonis.osti.gov

Available for sale to the public, in paper, from:

U.S. Department of Commerce
National Technical Information Service
5285 Port Royal Road
Springfield, VA 22161
phone: 800.553.6847
fax: 703.605.6900
email: orders@ntis.fedworld.gov
online ordering: http://www.ntis.gov/help/ordermethods.aspx

Cover Photos: (left to right) photo by Pat Corkery, NREL 16416, photo from SunEdison, NREL 17423, photo by Pat Corkery, NREL 16560, photo by Dennis Schroeder, NREL 17613, photo by Dean Armstrong, NREL 17436, photo by Pat Corkery, NREL 17721.

Printed on paper containing at least 50% wastepaper, including 10% post consumer waste.

Acknowledgments

This work was supported by the U.S. Department of Energy under contract number DE-AC36-08GO28308 with the National Renewable Energy Laboratory. The authors would like to thank Dr. Donald Houser and Jason Austin of The Ohio State University for their finite element modeling support.

List of Acronyms

C	Celsius
CRB	cylindrical roller bearing
DAS	data acquisition system
GB	gearbox
GRC	Gearbox Reliability Collaborative
HS	high speed
HSS	high speed shaft
Hz	hertz
kN	kiloNewtons
mm	millimeter
με	microstrain
μm	micrometer
NI	National Instruments
NREL	National Renewable Energy Laboratory
NWTC	National Wind Technology Center
R^2	coefficient of determination
RCS	remote control screen
RTD	resistance temperature detector
SOP	safe operating procedure
TRB	tapered roller bearing
V	Volt

Table of Contents

List of Figures

List of Tables

1 Introduction

The National Renewable Energy Laboratory (NREL) Gearbox Reliability Collaborative (GRC) is a project investigating gearbox reliability primarily through testing and modeling. Previous dynamometer testing focused upon acquiring measurements in the planetary section of the test gearbox [1]. Prior to these tests, the strain gages installed on the planetary bearings were calibrated in a load frame [2].

Recent input from GRC participants has highlighted the need for measurements of gear and bearing response, including reactions, load distributions, and temperatures in the high speed (HS) section of the gearbox due to a high rate of failures in the locating bearings supporting the high speed shaft (HSS) [3]. Thus, instrumentation has been added to the HSS, pinion, and tapered roller bearing (TRB) pair of the GRC gearbox (GB) to measure loads and temperatures. A portion of the upcoming GRC dynamometer test program will then measure these loads in test conditions, including normal operation, generator radial misalignment, and simulated emergency stop conditions [4].

The new HSS instrumentation on the TRB pair was calibrated from May 22–24, 2013, prior to starting the planned dynamometer tests. The purpose of this document is to describe this calibration process for the TRB pair instrumentation and the test results.

2 Test Bearings

2.1 Description and Modifications

The test articles are the instrumented TRB pair for GRC GB #2. Both bearings are type SKF 32222 J2 tapered roller bearings. The TRB is 200 millimeters (mm) in outer diameter, with a bore of 110 mm and a total length of 56 mm. It has 20 rolling elements at a 16° taper angle and weighs approximately 20 pounds. The radial static load capacity of the bearing is 570 kiloNewtons (kN) (128 kip) [5].

In operation, the HSS is supported on its upwind end by a cylindrical roller bearing (CRB) and near its midpoint by the TRB pair. The TRB pair is mounted in an o-configuration, which provides greater tilt stiffness than the x-configuration, and the TRBs are separated by a pair of spacers. Each of these bearings is supported within parts of the housing casting, notably the "cone" supporting the TRB pair. A locknut on the shaft provides the clamping force to retain the preload in the TRBs. The bearing outer rings are retained by an end cap, which is bolted to the exterior of the housing. The end cap reacts the axial loads imparted at the pinion. The entire HSS assembly and gearbox housing are shown in Figure 1.

The HSS assembly was removed from GB #2 in November 2012. During the removal, the existing TRB pair was slightly damaged, preventing reuse. A new TRB pair was purchased and then machined in January 2013 to facilitate the installation of the instrumentation. Four equally spaced axial grooves were machined in the outer ring of each TRB. Each groove is cut at an angle that matches the taper angle of the outer ring, with a maximum depth of 10 mm at the thick end and a width of 15 mm. The axial grooves allow for the actual placement of the gages, but also serve the purpose of increasing the local strain field to improve gauge response. A 5 mm wide by 4.2 mm deep circumferential groove was also machined in the outer ring to allow for routing of the wiring to one location, which serves as the exit point from the bearing face and out through the gearbox housing. Finally, a small hole was machined in the thick end of each outer race such that a pin could be installed between each bearing, serving as a key.

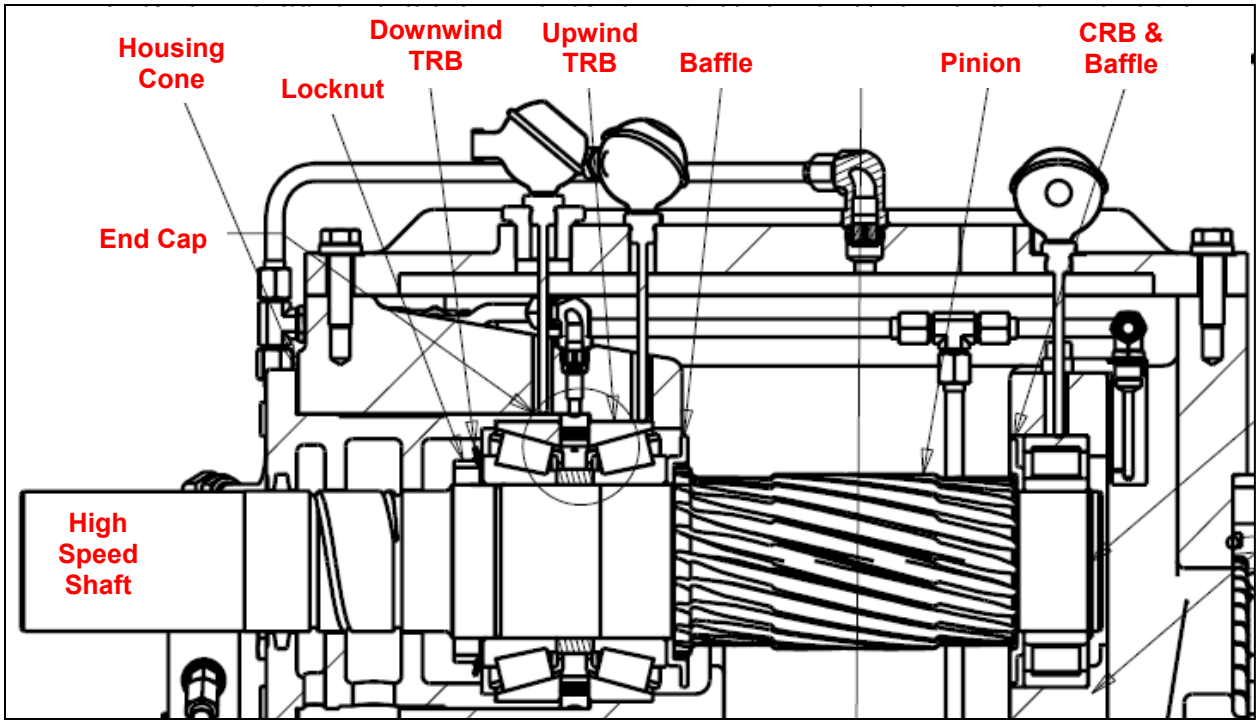

Figure 1. Schematic of high-speed shaft installation in the gearbox. ***Illustration by Powertrain Engineers Inc.***

2.2 Instrumentation

The instrumentation, listed in Table 1, was installed on the TRBs in March 2013. Strain gages on the TRB outer rings measure radial loads, as shown in Figure 2 and Figure 3. The data sheet for the strain gages is shown in Figure 4. Gage pairs are located at two different axial locations in each of the four grooves for a total of eight gage pairs per bearing. They are wired in a Poisson half-bridge configuration. Additionally, a resistance temperature detector (RTD) measures the outer ring temperature of each TRB, as shown in Figure 5. The instrumentation package installed on the topmost groove of the downwind TRB is shown in Figure 6. Finally, the gages and RTDs, along with the wires in the circumferential grooves, were glued together and to the bearing for environmental protection, as shown in Figure 7.

The installed strain gages measure the strain in the remaining "bridge" of bearing race material as the rollers move underneath it and deflect it. Finite element modeling was employed to determine the groove dimensions to result in an appreciable strain field in the remaining bridge material [6]. The two axial locations provide an indication of the load distribution across the axial width of the ring. The axial locations were selected to be well within the contact area between the roller and ring, while still providing enough room for the wires between the ring and the gearbox housing. The four circumferential locations provide a coarse indication of the load distribution around the bearing outer ring. Instrumenting both the upwind and downwind TRBs, of course, gives an indication of the load share between bearings.

Table 1. TRB Calibration Instrumentation

Part	Derived Measurement	Label	Sensor
Upwind TRB	Strain, 0°, thin end	TRB_Up_00_A	Vishay CEA-06-062UT-350
Upwind TRB	Strain, 0°, thick end	TRB_Up_00_B	Vishay CEA-06-062UT-350
Upwind TRB	Strain, 90°, thin end	TRB_Up_90_A	Vishay CEA-06-062UT-350
Upwind TRB	Strain, 90°, thick end	TRB_Up_90_B	Vishay CEA-06-062UT-350
Upwind TRB	Strain, 180°, thin end	TRB_Up_180_A	Vishay CEA-06-062UT-350
Upwind TRB	Strain, 180°, thick end	TRB_Up_180_B	Vishay CEA-06-062UT-350
Upwind TRB	Strain, 270°, thin end	TRB_Up_270_A	Vishay CEA-06-062UT-350
Upwind TRB	Strain, 270°, thick end	TRB_Up_270_B	Vishay CEA-06-062UT-350
Upwind TRB	Outer ring temperature	TEMP_TRB_Up	Omega SA1-RTD-120
Downwind TRB	Strain, 0°, thin end	TRB_Dwn_00_D	Vishay CEA-06-062UT-350
Downwind TRB	Strain, 0°, thick end	TRB_Dwn_00_C	Vishay CEA-06-062UT-350
Downwind TRB	Strain, 90°, thin end	TRB_Dwn_90_D	Vishay CEA-06-062UT-350
Downwind TRB	Strain, 90°, thick end	TRB_Dwn_90_C	Vishay CEA-06-062UT-350
Downwind TRB	Strain, 180°, thin end	TRB_Dwn_180_D	Vishay CEA-06-062UT-350
Downwind TRB	Strain, 180°, thick end	TRB_Dwn_180_C	Vishay CEA-06-062UT-350
Downwind TRB	Strain, 270°, thin end	TRB_Dwn_270_D	Vishay CEA-06-062UT-350
Downwind TRB	Strain, 270°, thick end	TRB_Dwn_270_C	Vishay CEA-06-062UT-350
Downwind TRB	Outer ring temperature	TEMP_TRB_Dwn	Omega SA1-RTD-120

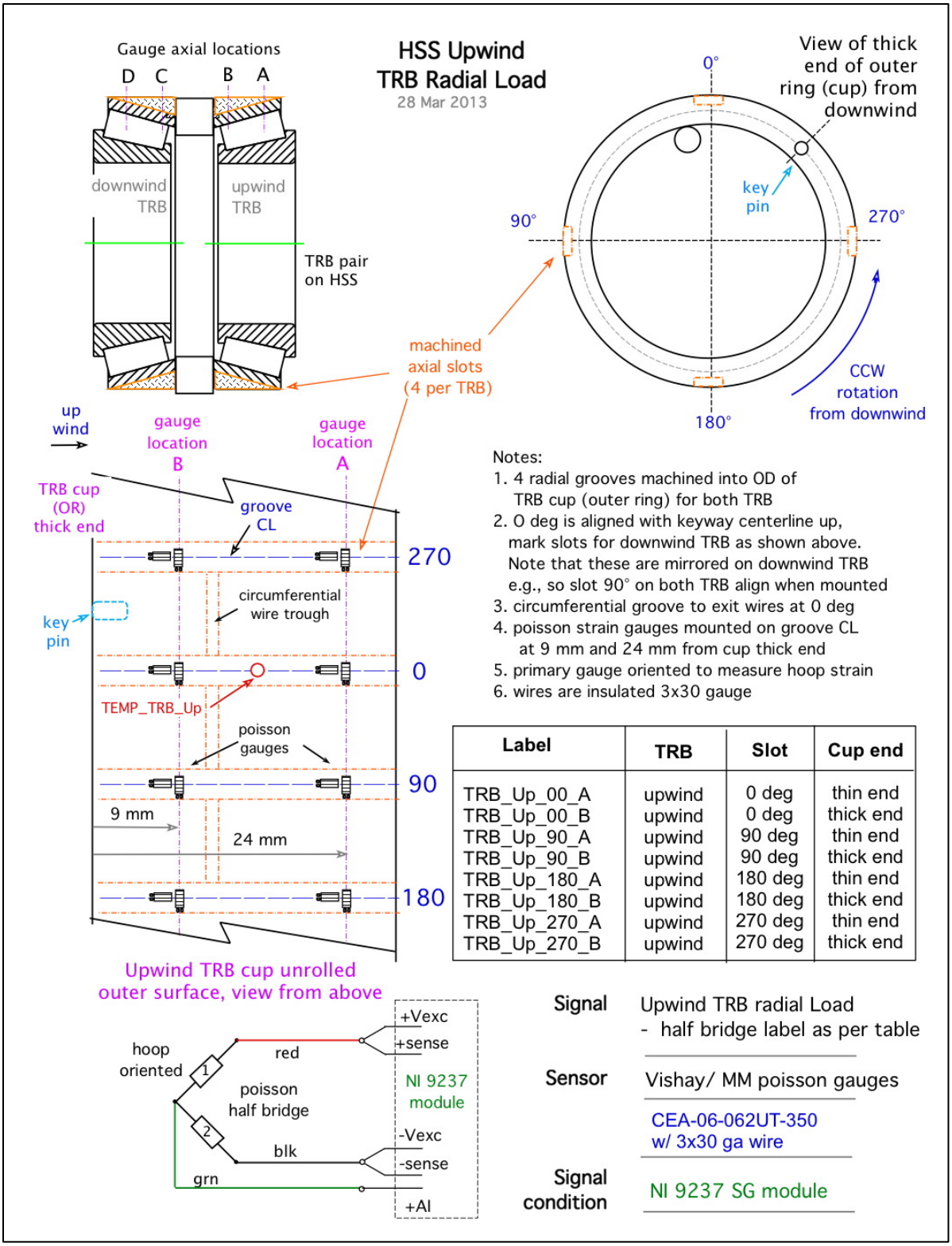

Label	TRB	Slot	Cup end
TRB_Up_00_A	upwind	0 deg	thin end
TRB_Up_00_B	upwind	0 deg	thick end
TRB_Up_90_A	upwind	90 deg	thin end
TRB_Up_90_B	upwind	90 deg	thick end
TRB_Up_180_A	upwind	180 deg	thin end
TRB_Up_180_B	upwind	180 deg	thick end
TRB_Up_270_A	upwind	270 deg	thin end
TRB_Up_270_B	upwind	270 deg	thick end

Figure 2. Upwind tapered roller bearing strain
Source: McNiff Light Industry

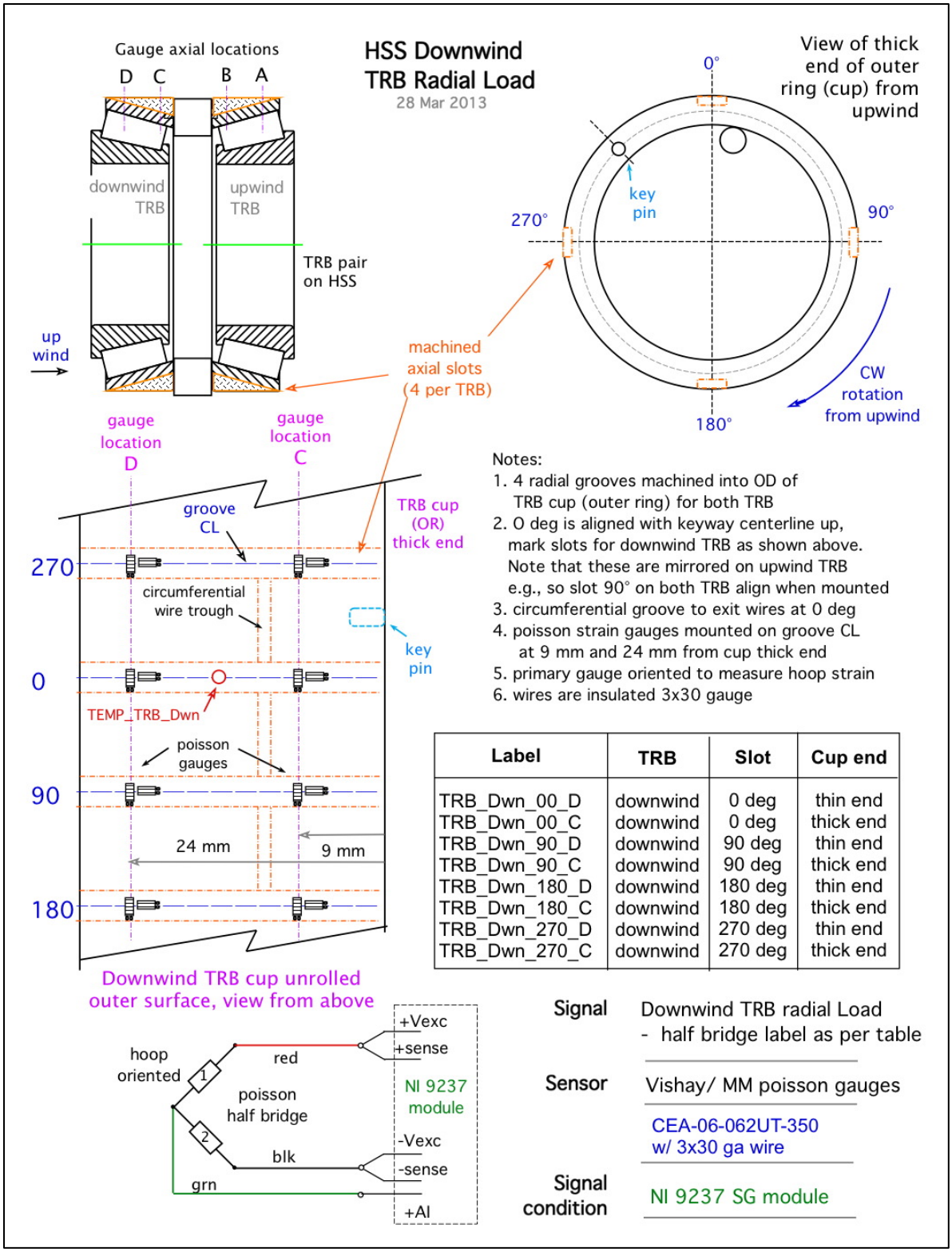

Label	TRB	Slot	Cup end
TRB_Dwn_00_D	downwind	0 deg	thin end
TRB_Dwn_00_C	downwind	0 deg	thick end
TRB_Dwn_90_D	downwind	90 deg	thin end
TRB_Dwn_90_C	downwind	90 deg	thick end
TRB_Dwn_180_D	downwind	180 deg	thin end
TRB_Dwn_180_C	downwind	180 deg	thick end
TRB_Dwn_270_D	downwind	270 deg	thin end
TRB_Dwn_270_C	downwind	270 deg	thick end

Figure 3. Downwind tapered roller bearing strain
Source: McNiff Light Industry

VISHAY PRECISION GROUP

062UT

Micro-Measurements

General Purpose Strain Gages - Tee Rosette

GAGE PATTERN DATA

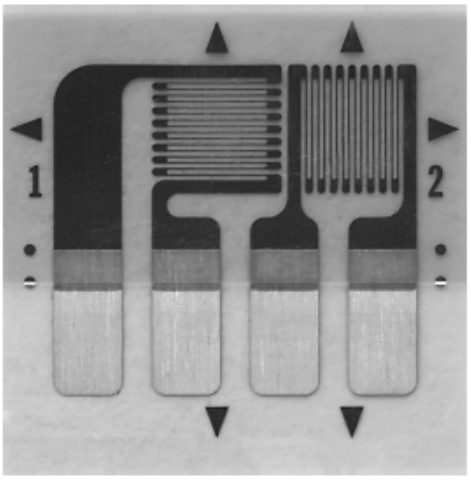

actual size

GAGE DESIGNATION See Note 1	RESISTANCE (OHMS)	OPTIONS AVAILABLE See Note 2
CEA-XX-062UT-120	120 ± 0.4%	**P2**
CEA-XX-062UT-350	350 ± 0.4%	**P2**

DESCRIPTION

Small general-purpose two-element 90° tee rosette. Exposed solder tab area 0.07 x 0.04 in [1.8 x 1.0 mm].

GAGE DIMENSIONS

Legend: ES = Each Section; S = Section (S1 = Sec 1); CP = Complete Pattern; M = Matrix

inch
millimeter

Gage Length	Overall Length	Grid Width	Overall Width	Matrix Length	Matrix Width
0.062 ES	0.205 CP	0.080 ES	0.225 CP	0.31	0.31
1.57 ES	5.21 CP	2.03 ES	5.72 CP	7.9	7.9

GAGE SERIES DATA

See Gage Series data sheet for complete specifications.

Series	Description	Strain Range	Temperature Range
CEA	Universal general-purpose strain gages.	±3%	–100° to +350°F [–75° to +175°C]

Note 1: Insert desired S-T-C number in spaces marked XX.

Note 2: Products with designations and options shown in bold are not RoHS compliant.

Figure 4. Strain gage data sheet
Source: Vishay Precision Group (http://www.vishaypg.com/docs/11125/062ut.pdf)

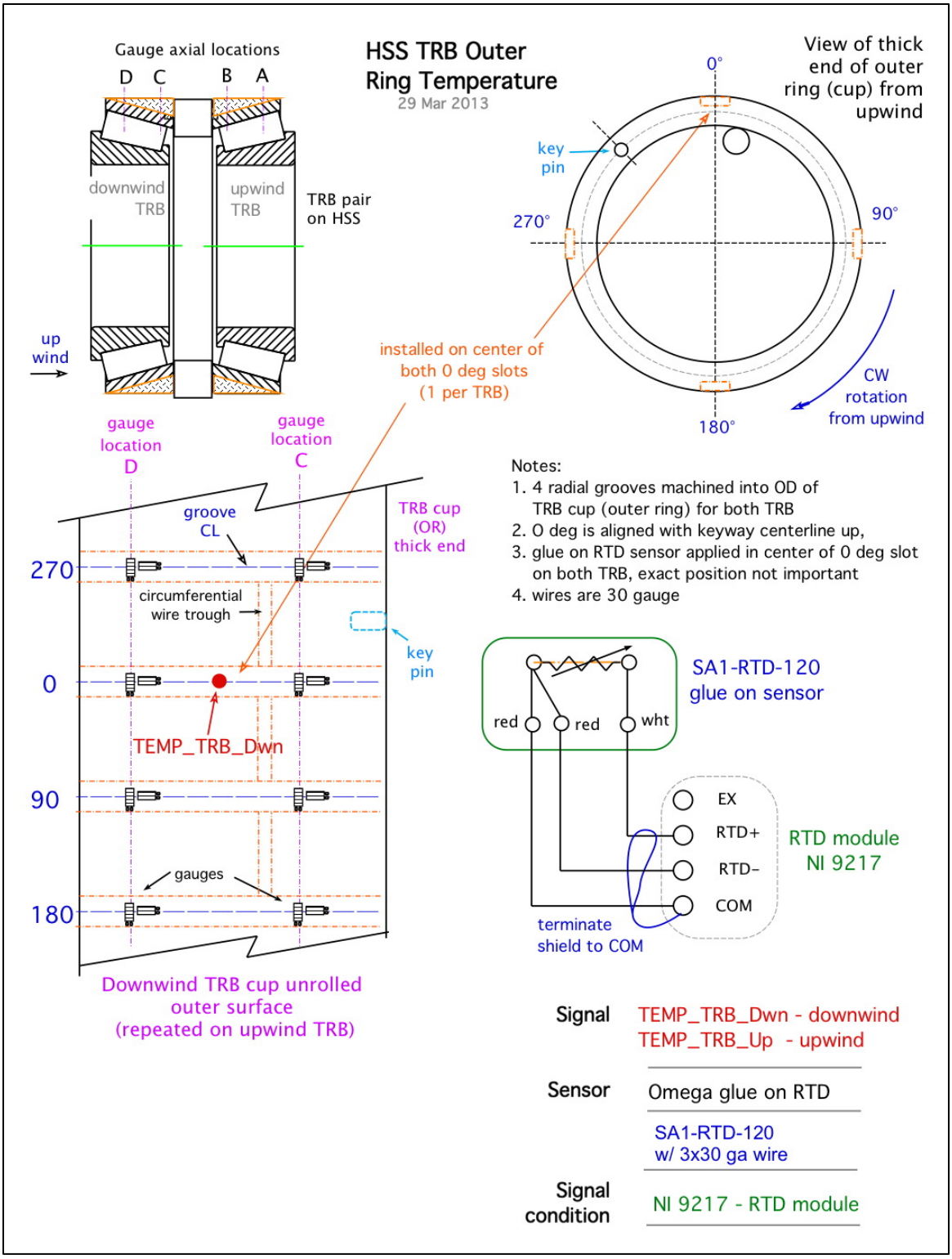

Figure 5. Bearing outer ring temperature
Source: McNiff Light Industry

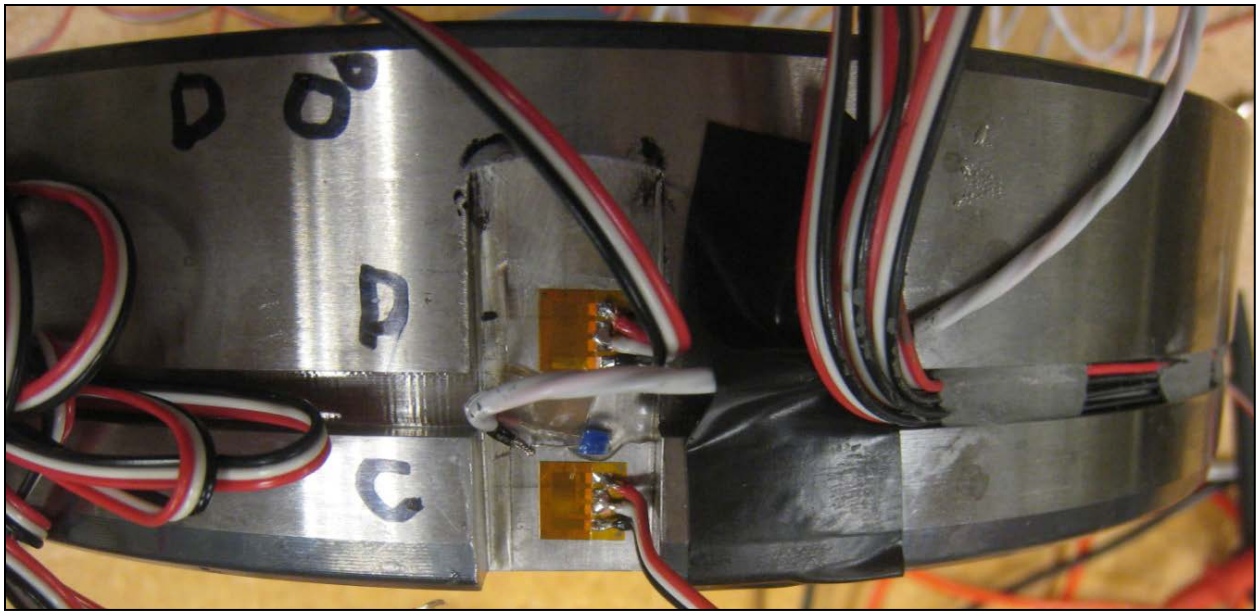

Figure 6. Bearing instrumentation before protection. ***Photo by Scott Naucler, NREL 26259***

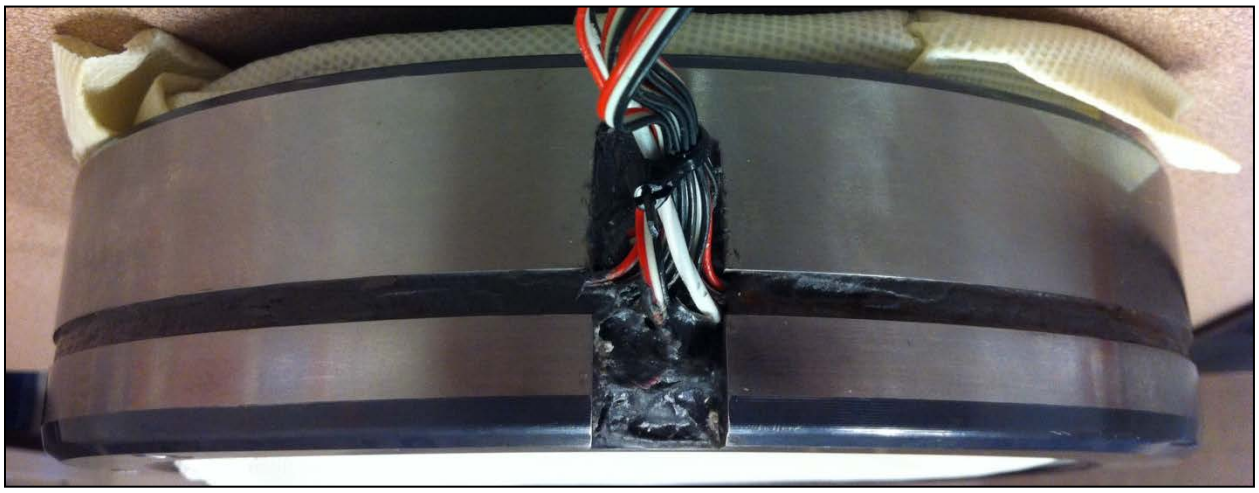

Figure 7. Bearing instrumentation after protection. ***Photo by Jonathan Keller, NREL 26257***

2.3 Calibration Requirements

Calibration requirements are different for the different sensors. The strain gages require direct signal-to-force calibration, necessitating a special test rig. The RTDs do not require calibration.

2.3.1 No Calibration

The RTDs installed on the TRB outer rings do not require calibration because they meet the RT100 specification. These devices are connected to special RTD specific modules in the data acquisition system (DAS), and they are recorded in units of degrees Celsius.

2.3.2 Direct Calibration

In the case of these strain gages, the data of interest is the absolute magnitude of load at each gage location. This measured load can then be compared to predictions in commercial modeling

software. Differences in the load distribution around the circumference, across the bearing face, and between the upwind and downwind TRBs are all of interest. In the ideal design and operational scenario, the loads would be shared equally in all of these areas. However, the combination of axial and radial loads from the pinion gear mesh, and the close spacing of the TRB pair results in unequal load sharing. Additionally, manufacturing tolerances and external loads from the brake disk or generator misalignment can further disrupt load sharing and result in a reduction in bearing life. Lastly, transient loads from the generator, such as a generator speed change or grid fault, are likely to disrupt load sharing and also result in a reduction in bearing life.

The desire for a measure of the absolute magnitude of load at each bearing gage location, along with the unique geometry of the bearing and groove necessitate direct calibration. The objective of this direct calibration is to measure the correlation between the load applied to the bearing and the strain gage response. The best method for calibration of the TRBs is to apply loads separately to each TRB while they are installed on a representative shaft. *In-situ* calibration of the TRBs was not possible, because there is no easy way to apply loads to the TRBs individually when the shaft is installed in the housing bore. Therefore, construction of a special test rig was required, which would facilitate application of loads individually to each TRB.

Furthermore, the test rig and loading mechanism must apply the load to the bearings in the axial direction rather than the radial direction. Either method would result in measurable strain on the TRB outer rings. However, applying a radial load would result in an unequal strain distribution around the circumference of the TRB. With only four measurement locations spaced around the circumference, translation of this unequal strain distribution to an equivalent load distribution would be problematic, if not impossible. Application of an axial load results in a nearly constant strain distribution around the circumference of the TRB. In this case, the axial load is transmitted through the bearing taper angle to the outer rings, resulting in an expansion of the outer ring, which is resisted by the housing (or test fixture). Only a portion of the axial load results in a radial load because of the taper angle; the majority of the axial load is reacted by the contact between the outer ring, spacer, and housing (or test fixture). A special test fixture was developed for that purpose and is described in the next section.

In operation in the GRC GB, the TRB pair reacts the axial and radial forces from the gear mesh and the shaft bending moments created by them. Modeling of the GRC GB predicts that at rated torque the bearing *pair* is loaded by axial and radial forces of 22 kN (5 kip) and 60 kN (13.5 kip), respectively. However, the bearings are not loaded equally around their circumference, nor are they loaded equally between the upwind and downwind rows [6]. A worst-case scenario would have only a portion of one bearing carrying all of these loads. In the course of this test, up to 50 kip of axial force was applied to each bearing. Through the 16° taper angle, this equates to a radial load of 61 kN (13.8 kip) distributed evenly around the bearing circumference. Thus, this test resulted in a radial load approximately equivalent to a worst case loading condition at rated torque in the gearbox.

3 Test Environment

The following sections describe the test equipment and setup.

3.1 Load Frame

The load frame used to calibrate the HSS TRBs was previously used to calibrate the GRC planet bearings [2] and is shown in Figure 8. It is located in the high bay of building 251 at the NWTC. It consists of a steel frame holding a 110 kip (444.8 kN) hydraulic actuator. The actuator is mounted on a crosshead assembly, which can be moved vertically through jackscrews. Once in the desired position, the crosshead is manually locked into position by tightening bolts around the load frame. In this manner, loads can be applied vertically downward to the test article from a variable height. The loads are then transmitted through the test article to a baseplate. The entire load frame is mounted to a large steel base with standard "t-slots." The base and t-slots are useful for mounting the required ancillary equipment, such as hydraulic pumps.

Control of the load frame is through an MTS Systems-designed controller using either a handheld remote control screen (RCS) device at the load frame itself or through a software program on a dedicated computer in a separate control room. In either case, the load frame can be operated in either load or displacement control modes. In load control, a load is commanded, and the actuator displaces as much as required to achieve the desired load—up to a total of 6 inches of travel. In displacement control, a displacement is commanded, and the actuator applies as much force as required to achieve the desired displacement—up to 110 kip. Various safety settings can be configured on the dedicated computer, which range from notifying the operator that a limit has been exceeded to completely shutting down the load frame. In this test, very small displacement limits were configured along with a maximum compressive force of 55 kip.

Installed on the load frame are a calibrated load cell and a proximity sensor, which measure the applied load and resulting displacement of the actuator, as listed in Table 2. Calibration of these devices and the control system was performed by MTS in advance of testing.

Table 2. Load Frame Instrumentation

Instrument	Derived Measurement	Label	Sensor
Proximity probe	Axial displacement	Displacement	MTS 244-41
Load cell	Applied axial load	Force	MTS 661.23E-01

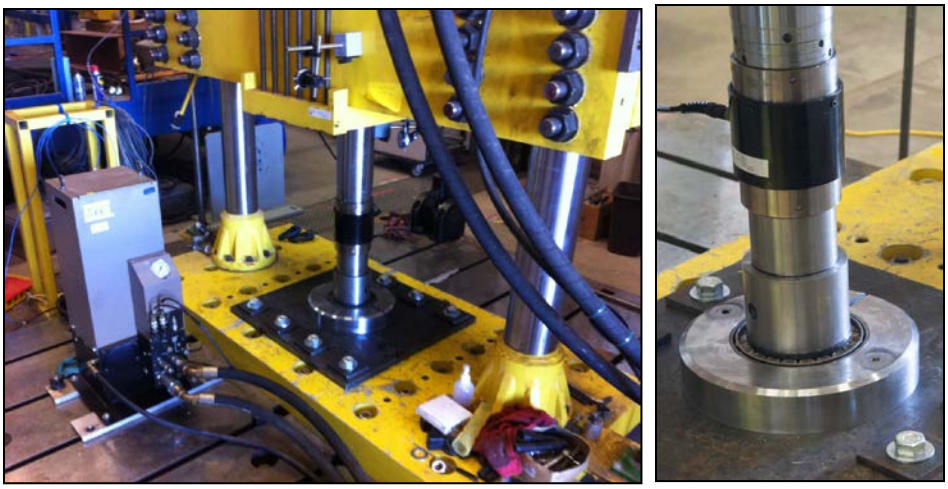

Figure 8. The 110-kip load frame (left) and test bearing (right). ***Photos by (left) Jonathan Keller, NREL 26258 and (right) Mark McDade, NREL 26260***

3.2 Bearing Calibration Fixture

A special calibration fixture, shown in Figure 9, was designed to support the instrumented TRB. An end cap is located at the top of the fixture. The end cap houses a Timken T200A thrust bearing, which allows for rotation of the TRB while under axial load. This permits the rolling elements to rotate directly under each individual groove in the outer ring. The thrust bearing mates with a shaft plug, which simulates the HSS. The shaft plug has a shoulder in it, which transfers loads to the TRB inner ring. The plug also has a radial through-hole, which allows a rod to be inserted into the plug to turn it under load. The TRB itself is retained in a collar that simulates the gearbox housing and retains the bearing circumferentially and axially. The collar design specifies 20 to 47 μm of diametrical clearance with the TRB outer ring, identical to the specified range of diametrical clearance between the downwind TRB outer ring and the end cap which retains it in the gearbox itself (P/N 251347). The collar produced was reported to have a clearance of just over 20 micrometers (μm). The collar is recessed into the baseplate, which in turn is bolted to the load frame base plate. The sensor wires from the TRB exit a slot machined in the collar.

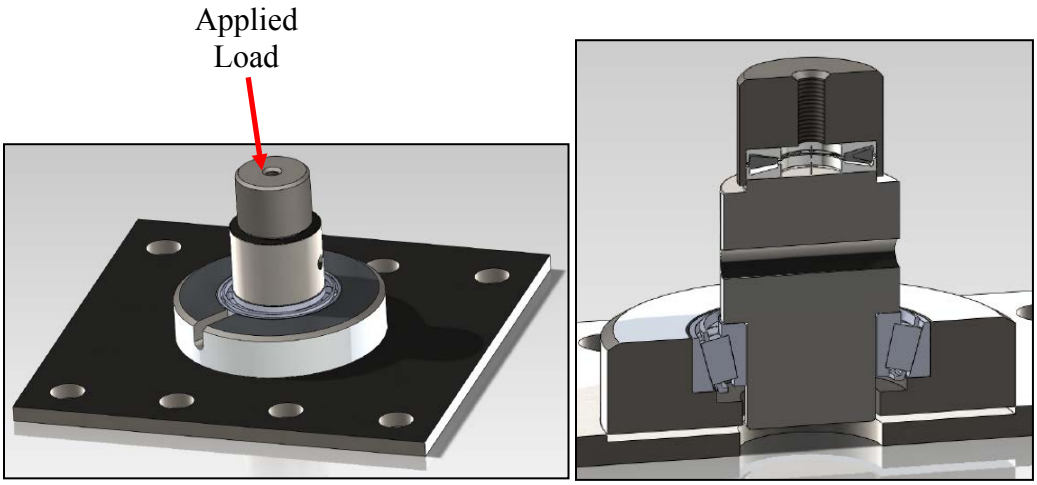

Figure 9. Bearing calibration fixture
Source: *Illustrations by Ed Overly, NREL*

3.3 Calibration Fixture Assembly

A schematic assembly of the complete fixture in the load frame is shown in Figure 10.

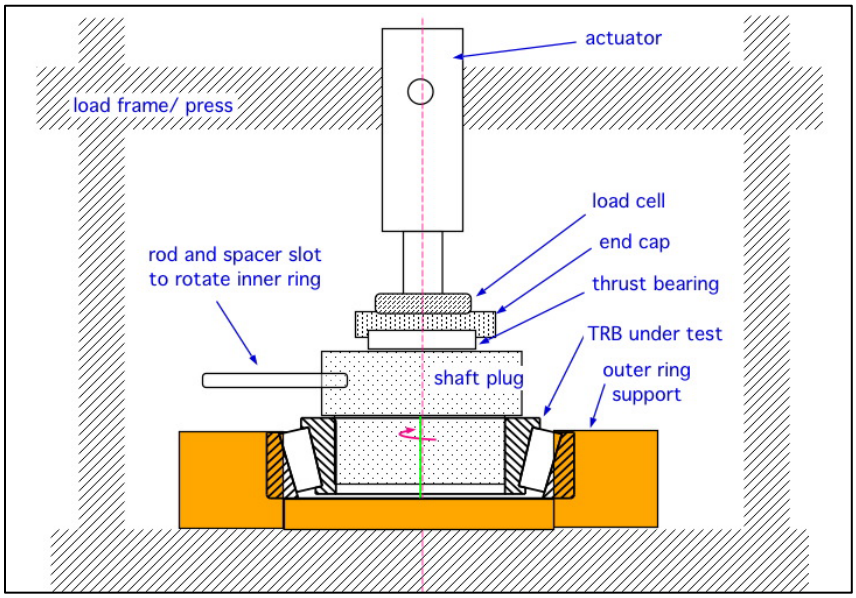

Figure 10. Completed calibration assembly
Source: McNiff Light Industry

3.4 Data Acquisition System

The DAS is based on the National Instruments (NI) deterministic Ethernet platform. Two NI 9237 signal-conditioning modules collected the eight strain gage half bridges and a NI 9217 signal-conditioning module collected the RTD signal. Additionally, the outputs of the load cell and axial displacement sensor on the load frame were brought into the DAS via Ethernet exchange with the MTS load frame controller. These signals were then sent through a NI PXI-1041Q chassis into the DAS computer. The data was displayed on screen for all channels. The strain gage channels were displayed and recorded in the native units of Volts per Volt (V/V) and also με, using a conversion factor of 366,300 derived from the gage factor and the Poisson arrangement. Temperature, actuator displacement, and force were displayed and recorded in units of degrees Celsius (C), inches, and kips, respectively.

The data files were named using the convention "TRB_UW_" or "TRB_DW_" and appended with "XX_YYYY_MM_DD_HH_SS_ZZZHz.tdms," where XX is the load in kips as measured by the load cell; YYYY, MM, DD, HH, and SS are the year, month, date, hour, and second of the data acquisition; and ZZZ is the data acquisition rate in hertz (Hz).

4 Test Sequence

This section describes the calibration process. Each TRB was calibrated separately.

4.1 Temperature Sensitivity Tests

Pretest measurements were acquired while the bearing outer ring was separated from the inner ring and rollers, and completely unloaded. The outer ring was heated to assess the effect of temperature on the measured strain value. The bearing was wrapped in an electric "barrel" heater and strain values were measured with the temperature ranging from ambient to 45°C. Data was acquired for a total of 60 seconds at 10 Hz, yielding data records of 600 points.

4.2 Load Calibration Tests

This section describes the set of tests to determine the correlation between radial load and measured strain. Setup and routine operation of the load frame was in accordance with an existing safe operating procedure (SOP) [7].

The actuator was placed in displacement control to slowly lower it until it came in contact with the end cap. At that point, the actuator was placed in force control for the remainder of the test. Loads were then applied in five kip increments up to 50 kip. At each increment, the bearing inner ring was rotated 180° in approximately five seconds to ensure that a minimum of three rollers pass under each groove. Data was acquired for a total of 20 seconds at 500 Hz, yielding data records of 10,000 points. Two acquisitions were acquired at each load level to assess repeatability. Upon reaching the maximum load, the process was reversed again, performing two acquisitions at each load level—yielding a total of four acquisitions at each load level.

5 Data Analysis

5.1 Temperature Sensitivity Analysis

The effect of temperature on the static output of all gages for the downwind bearing is shown in Figure 11. Ambient temperature the day of the test was 24°C. The maximum temperature the bearing was heated to by the "barrel" heater was 45°C. Over this range, the strain increased by approximately 5 μV/V, or 2 με, for each gage pair. This change in strain is small compared to the strains experienced under the axial loading tests representative of operational loads described in the following sections.

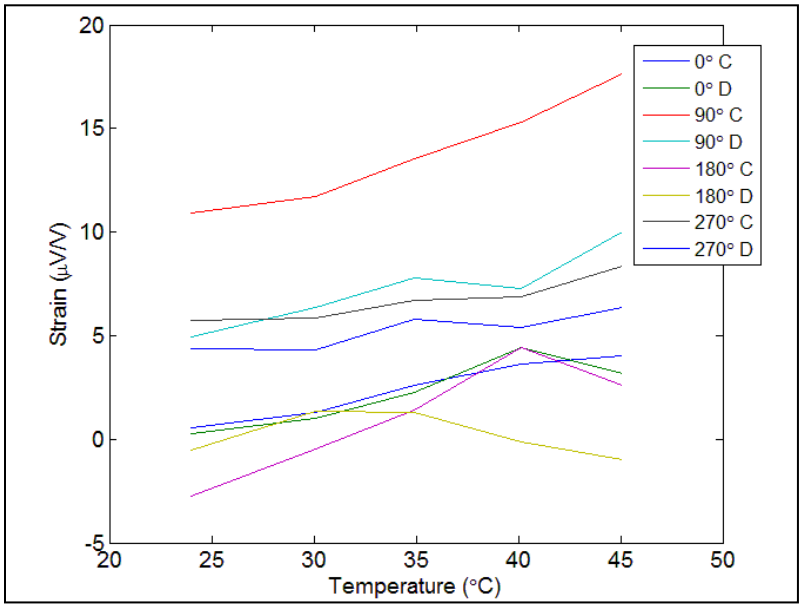

Figure 11. Effect of temperature on measured strain

5.2 Load Calibration Analysis

Gage calibration is determined from the measured data by regression analysis of the gage response to the applied load. The analysis process and final results are discussed in the following subsections.

5.2.1 Example Gage and Applied Load Responses

Figure 12 shows example acquisitions for the TRB_Up_00_A channel (upwind bearing, 0° groove, thin end) at applied loads of 25 and 50 kip. Only the first 10 seconds of the acquisition are shown for clarity. The strain gage response has been displayed in units of μV/V for ease of interpretation. True strain values are also given throughout the text for reference; however, for the purpose of future dynamometer testing, the relationship of interest is really between the applied load (kip) and strain gage response (V/V). The intermediate step of converting strain gage response (V/V) to true strain (με) is not necessary.

Both signals are composed of three regions. The first is an initial, steady level. Then at approximately $t = 2$ seconds, the bearing was rotated 180° by hand over a period of 3 to 5 seconds, resulting in a sinusoidal behavior in the measured strain gage response. During this

period, the load fluctuates only slightly, but the strain gage response changes dramatically. The strain gage response is composed of three to four approximate sine waves, which correspond to three or four rollers passing underneath the gage pair. At the conclusion of the rotation, the strain gage response returns to a final, steady level.

There are several interesting characteristics of the responses. Firstly, the applied load in each case is relatively constant as desired. During the rotation, it varies less than ± 0.2 kip, which is less than 1% of the applied load. Turning to the strain gage response, note that the initial and final strain gage response values are highly dependent upon the roller position relative to the strain gage pair. The initial strain gage response is approximately -1000 μV/V for both of these cases, although the applied load has been doubled. Thus, the mean must be assessed from the sinusoid itself, rather than the initial or final responses, which have little intrinsic value. At 25 kip, the mean strain gage response is approximately -950 μV/V (348 με); at 50 kip, the mean strain gage response is approximately -1250 μV/V (458 με). This mean strain gage response can be thought of as a result of the hoop stress within the bearing due to the applied axial force and the bearing taper angle.

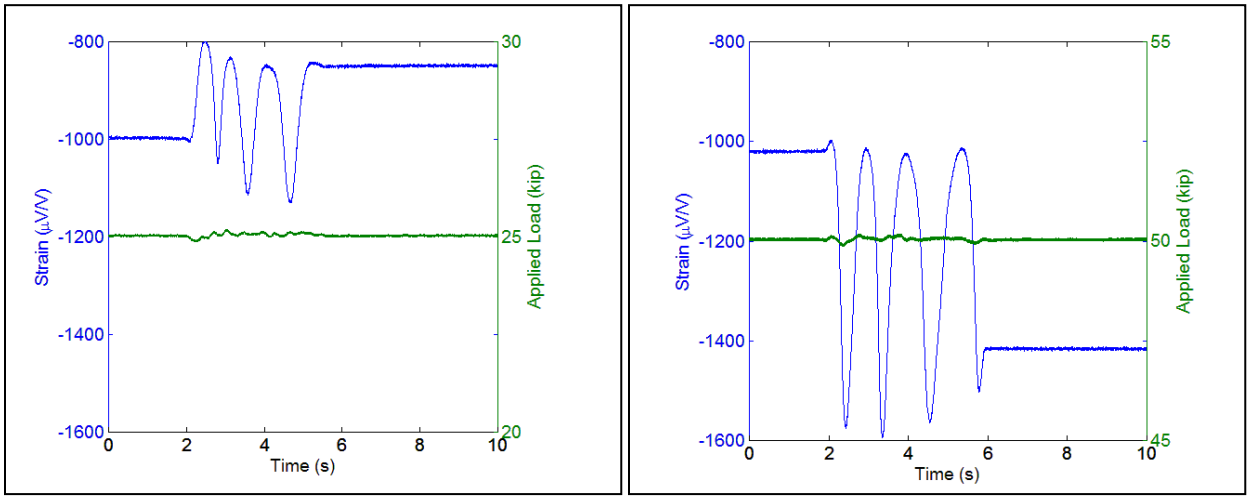

Figure 12. Measured load and strain for upwind bearing at 0° groove in thin end at 25 kip (left) and 50 kip (right)

Within the sinusoidal region during the rotation of the bearing, the peaks occur when two rolling elements are equally spaced away from the gage pair as shown in Figure 13. The valleys in the response occur when a rolling element is located directly under the groove and gage pair axis. This behavior was visually confirmed during the course of the test and can be thought of as a result of the flexure of the remaining 'bridge" of material in the bearing groove where the strain gage pair is located. The flexure of the bridge is highly dependent upon the location of the rollers beneath it, as illustrated in Figure 13. When the rollers are equidistant from the groove, the bearing radial forces bend the bridge of material downward, resulting in a compressive bending condition measured by the gage, which reduces the total stress. When the roller is directly under the groove, the bearing radial force bends the bridge of material upward, resulting in a tensile bending condition measured by the gage, which is additive to the mean hoop stress.

At 25 kip, the range (peak-to-valley) of the sinusoid is approximately 300 μV/V (110 με); at 50 kip, the range is approximately 600 μV/V (220 με). Note that strains of this magnitude, 100 to

200 με, can be measured very accurately by the strain gages. Thus, the grooves function as intended, resulting in measurable strain values as predicted by finite element modeling.

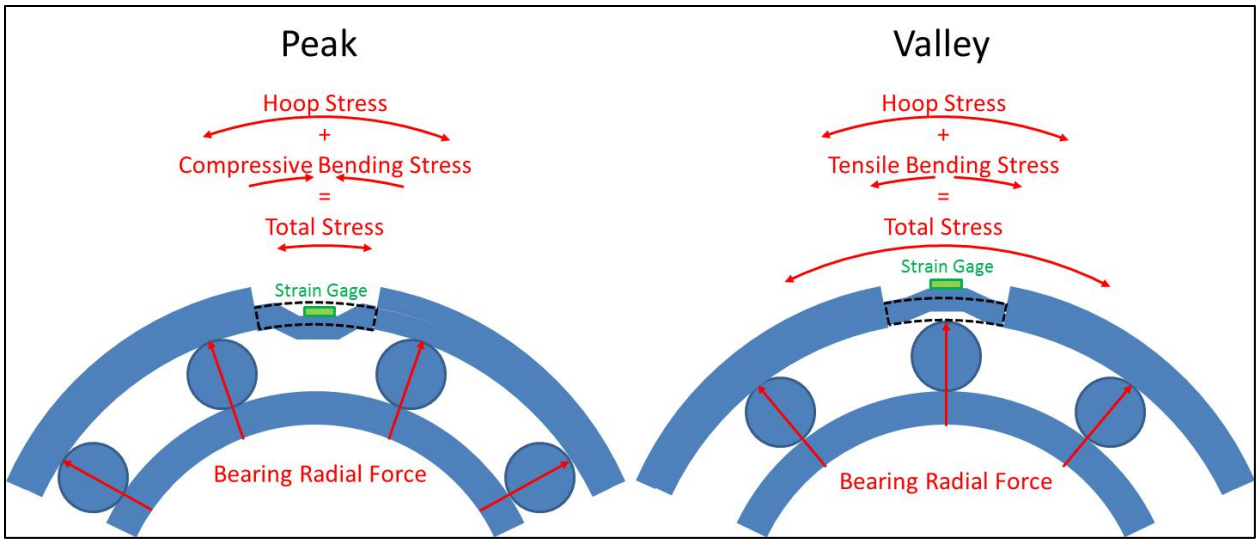

Figure 13. Rolling element positions at signal maximum and minimum

As seen in the responses, there are some variations in the magnitudes of the individual peaks and valleys for each roller, especially at the lower applied load level. Thus, when reducing the data, it is best to define a mean and a range by averaging the peaks and valleys for each acquisition as discussed in the following section.

5.2.2 Gage and Applied Load Data Processing

The data for each gage pair at each load level was post-processed to calculate the mean and range. In this process, additional steps were required to de-noise the data and are outlined as follows.

1. A 10 Hz, a low-pass filter is applied to de-noise the data originally acquired at 500 Hz.
2. The individual valleys (time index from start of data set) are then located using first and second derivatives and accounting for slip, duplicated valleys, and half periods. Using the individual valleys allows the identification of each sinusoid in the response.
3. For each sinusoidal period identified:
   - The mean applied load for the period is the mathematical average of the load cell output in the period.
   - The mean of the strain gage response for the period is the mathematical average of strain gage response in the period.
   - The range of the strain gage response for the period is determined by subtracting the maximum strain response from the minimum strain response within the period.
4. For each acquisition containing multiple sinusoidal periods:
   - The mean applied load for the acquisition is the mathematical average of the mean applied load for each period.

- The mean of the strain gage response for the acquisition is the mathematical average of the mean of the strain gage response for each period.
- The range of the strain gage response for the acquisition is the mathematical average of the range of the strain gage response for each period.

5.2.3 Example Gage and Applied Load Regression Analysis

Once the mean applied load, mean of the strain gage response, and range of the strain gage response were calculated for each acquisition, a regression analysis was completed as outlined in the following sections. The desired outcome of the regression analysis is a linear correlation between the applied load and some strain gage response characteristic. For previous GRC calibration of planet bearings, the range of the strain gage response provided the best correlation with applied load [2]. For this activity, regression analyses were performed for both the mean and the range.

Figure 14 shows the results of the regression analysis for just the TRB_Up_00_A channel (upwind bearing, 0° groove, thin end). Regression analyses were performed for all channels on both bearings, but the results shown below are typical. For both the mean and the range, the strain gage response increases monotonically with applied load. However, the mean exhibits a bilinear response, whereas the range exhibits a linear response.

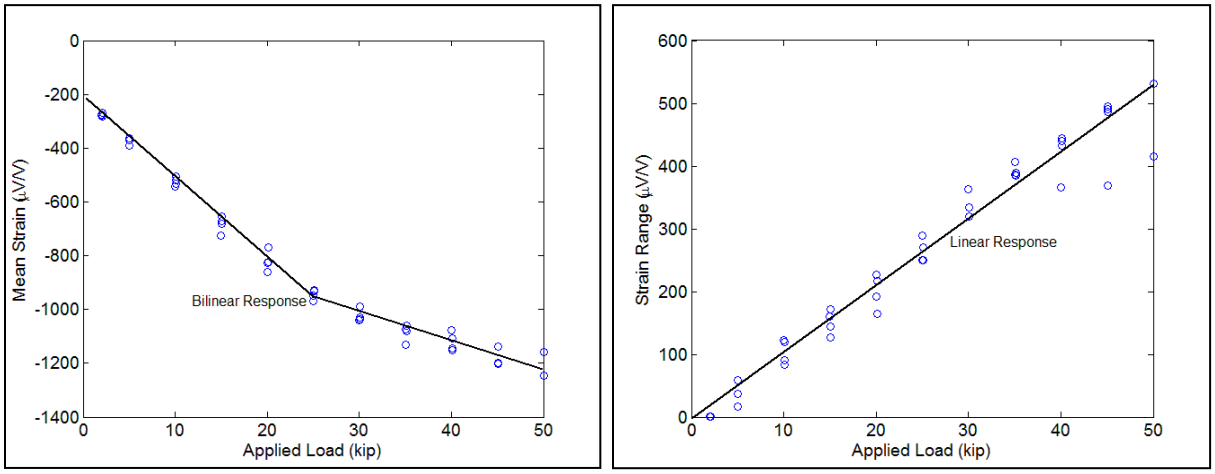

Figure 14. Regression analysis for upwind bearing at 0° groove in thin end, for mean (left) and range (right)

Up to an applied load of approximately 25 kip, the mean increases significantly with applied load, but after this point the mean increases much more slowly. Remember that the collar retaining the bearing was produced with just over 20 μm of diametrical clearance with the TRB outer ring. It is hypothesized that below 25 kip of applied load, the bearing outer ring has not yet been stretched diametrically enough to fill up this clearance; thus, the system stiffness is simply comprised of the outer ring stiffness. At 25 kip, the bearing outer ring becomes fully engaged with the steel collar. At this point, the system stiffness is now composed of both the outer ring stiffness and the steel collar stiffness. This relatively simple explanation describes the bilinear behavior in the mean strain.

There can be small differences in diametrical tolerances of the steel collar, the gearbox end cap (P/N 251347) that retains the downwind bearing, the gearbox bore that retains the upwind bearing, and any individual bearing. These tolerance differences would result in a difference in the diametrical clearance in each situation from 20 to 47 μm, and thus, a difference in the inflection point in the mean strain. Therefore, this bilinear behavior is undesirable for purposes of translating measured strain gage response to operating load in the planned gearbox tests.

Turning to the range of the strain gage response, note that it is not affected by this hypothesized change in system stiffness at 25 kip. It exhibits a linear response over its entire range. There are single data points at the 40, 45, and 50 kip applied loads that have lower range values than the other three data points; however, they are not representative of the overall trend. In general, the measured range at each applied load is relatively consistent. Using a linear curve fitting approach yields a coefficient of determination (R^2) value of 0.96 for this data set.

5.2.4 Full Regression Analysis Results

The regression analysis results for the range for the upwind bearing are shown in Figure 15.

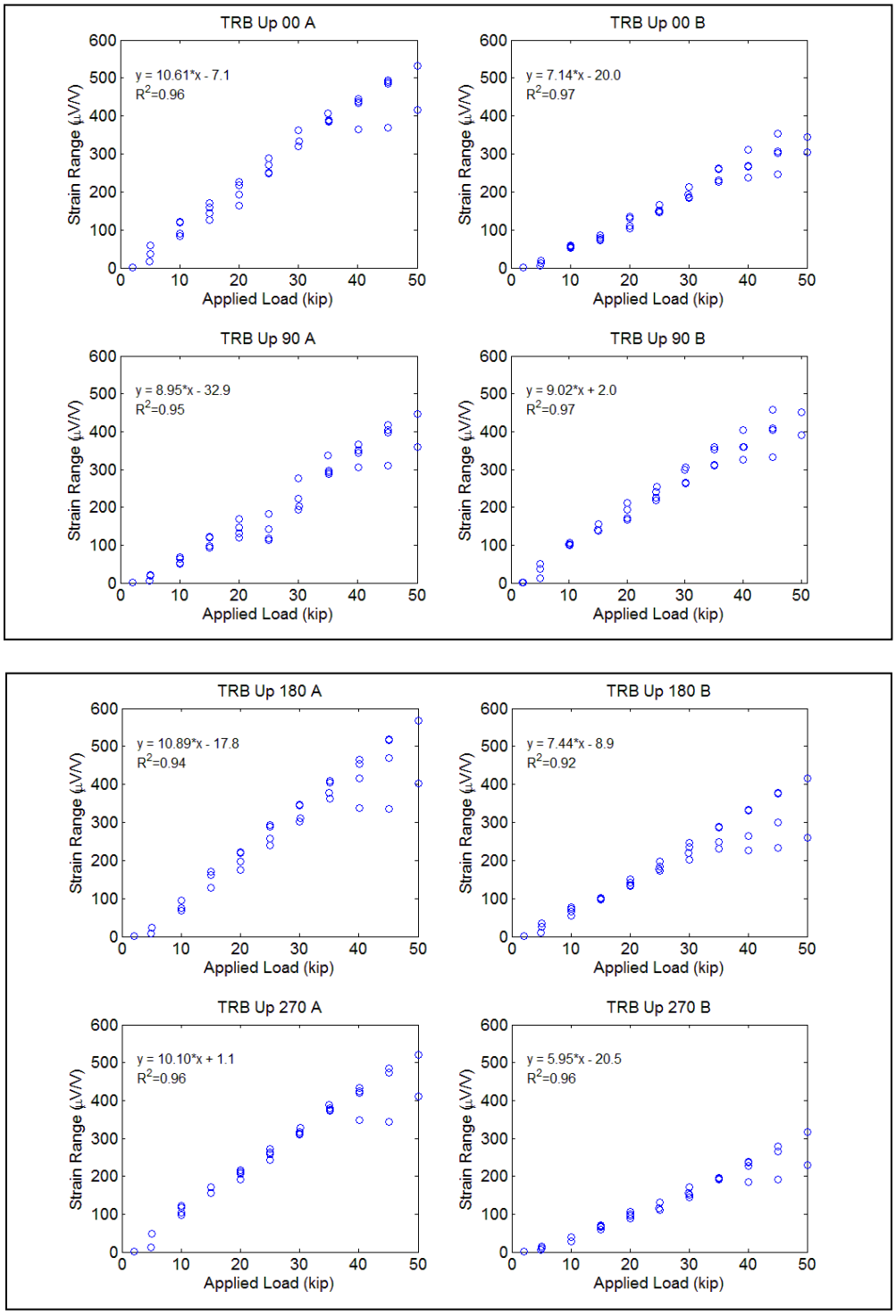

Figure 15. Regression analysis for upwind bearing

The regression analysis results for the range for the downwind bearing are shown in Figure 16.

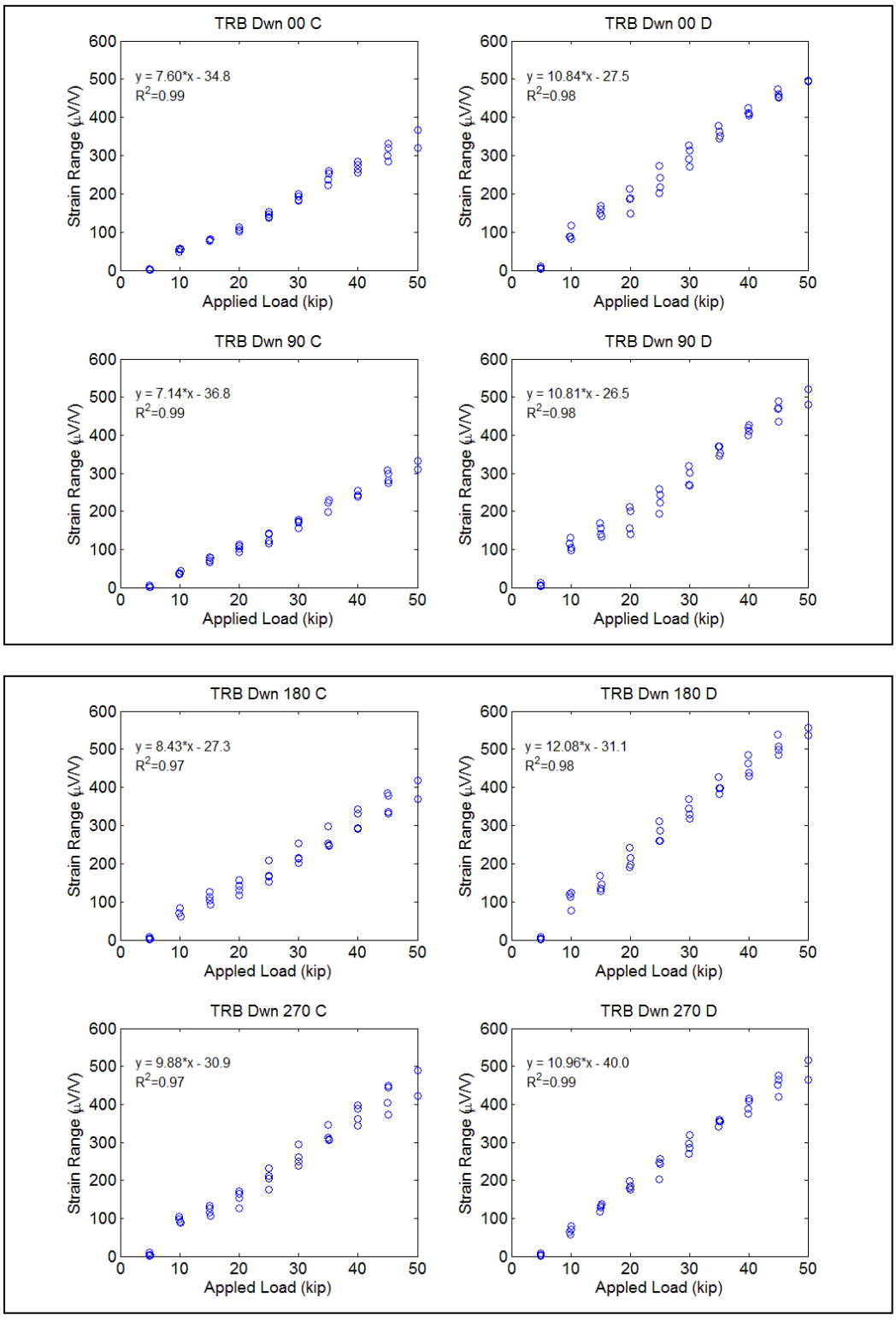

Figure 16. Regression analysis for downwind bearing

The results are more consistent for the downwind bearing, with a minimum R^2 value of 0.97, than the upwind bearing, with a minimum R^2 value of 0.92. For the upwind bearing, there are single acquisitions at the 40, 45, and 50 kip applied loads, which have lower range values than the other three acquisitions. The downwind bearing tests did not exhibit this behavior.

The sensitivity of each gage pair to applied load—that is, the slope of the linear correlation of range of the strain gage response—is also given in Figure 15 and Figure 16. For convenience, these sensitivities are shown all together in Figure 17. There are several trends that are of note. For any given axial position (A to D), it is expected the sensitivity around the circumference (0° to 270°) should be very similar given the grooves are machined with the same dimensions rather accurately, the gages are installed in the same location and orientation within the groove as closely as possible, and the load distribution around the circumference should be nearly circular. This expectation largely bears out. The best example of similarity is the gages on the downwind bearing, thin end (axial position D). Here, the average sensitivity is 11.2 μV/V/kip with the maximum being 8% greater than the average. The gages on the upwind bearing, thin end (axial position B) show the least similarity, where the average sensitivity is 7.4 μV/V/kip with the maximum being 22% greater than the average.

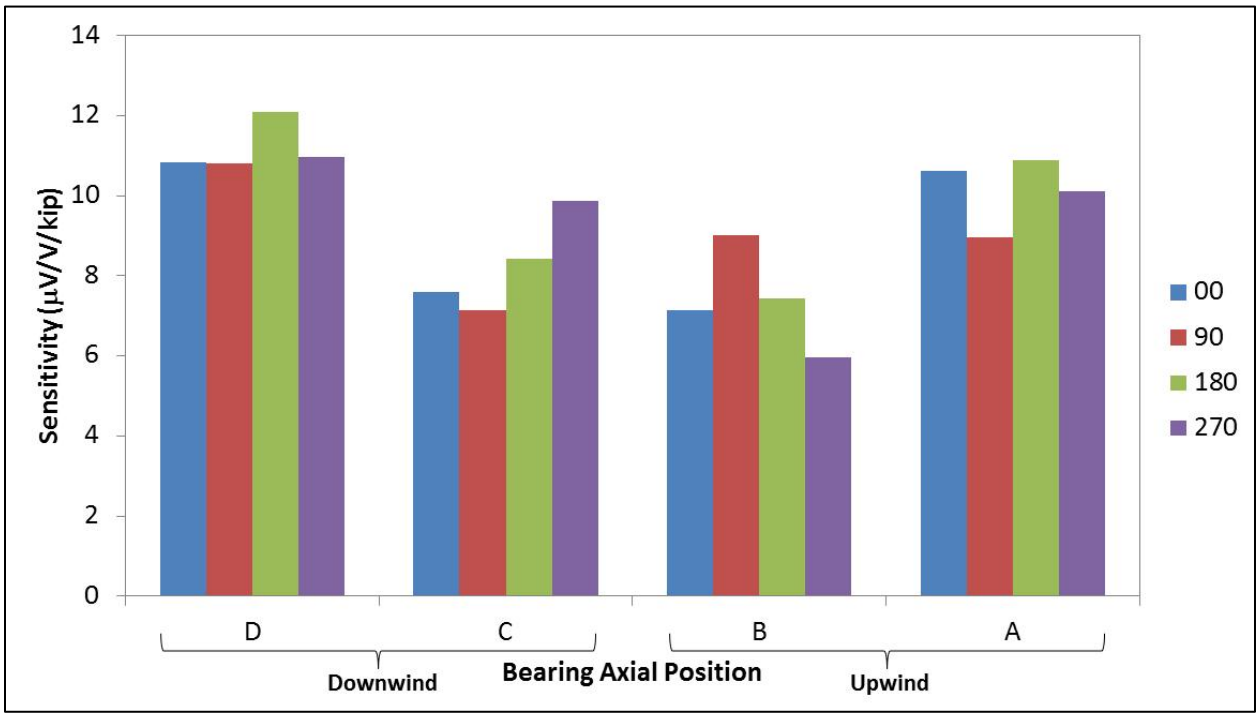

Figure 17. Calibration sensitivity comparison

The average sensitivities are 11.2, 8.3, 7.4, and 10.1 μV/V/kip for positions D, C, B, and A respectively. As expected, the sensitivities for the thin-end gages (D and A) should be similar and also greater than the thick-end gages (C and B). Regarding the differences in sensitivities around the circumference and between similar positions, referring back to Figure 6 shows that the strain gage occupies a sizeable portion of the groove in the bearing race. It is hypothesized that small differences in the gage position within the groove and orientation to the shaft axis result in slightly varying stiffness and response characteristics at the strain gages.

5.2.5 Final Calibration Coefficients

The calibration results discussed herein have thus far been in terms of applied axial load and resulting strain gage response. For the purposes of dynamometer testing, the range of the strain gage response will be measured for each gage pair. These measured ranges will then be used to calculate the radial, not axial, load at each position. Thus, the desired final result from this calibration exercise is the sensitivity of the range of the strain gage response in units of radial load per volt output of the Wheatstone bridge (kip/V/V). These final sensitivities are calculated in the following subsections. First, however, it is required to determine the component of the applied load acting at the gage axis.

5.2.5.1 Determining Applied Load

Although the load was applied to the test article along its axial (rotation) axis, as shown in Figure 18, the calibration objective is to determine the signal response proportional to radial load. The radial load, F_{radial}, is proportional to the load applied axially to the inner ring, $F_{applied}$, and the tangent of the taper angle ($\theta = 16°$):

$$F_{radial} = F_{applied} \tan\theta \,. \tag{1}$$

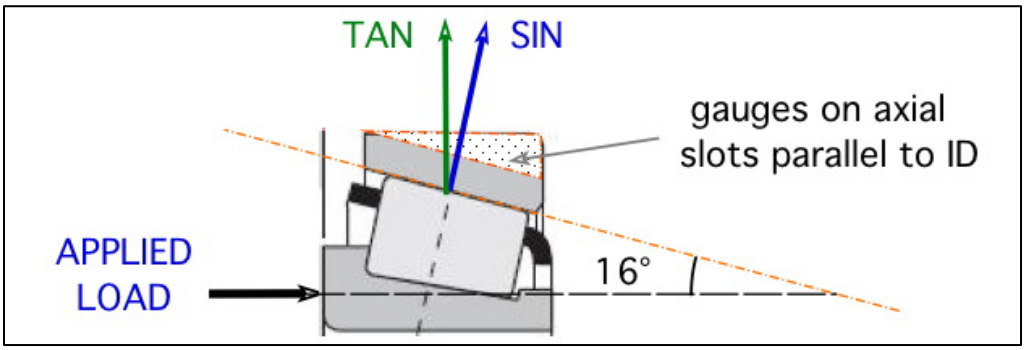

Figure 18. Load components
Source: McNiff Light Industry

The load at one roller, F_{roller}, as it goes over the gage axis, is the radial load divided by the number of rollers ($N_{roller} = 20$), assuming a circular load distribution. This roller load is the load the gage is responding to sinsusoidally:

$$F_{roller} = \frac{F_{radial}}{N_{roller}} \,. \tag{2}$$

In this situation, with only an axial load, this assumption is well justified within normal bearing manufacturing tolerances, and the proper alignment of the load frame and bearing. Regarding the influence of the grooves on the circular load distribution, finite element modeling also showed this assumption to be fairly well justified. Compared to a bearing without grooves, the rollers experienced a radial force of only 10% to 15% less than when directly under a groove in the modified bearing [6].

5.2.5.2 Calculated Calibration Coefficients

Table 3 and Table 4 list the final calibration coefficients, in terms of the measured sensitivity of the range of the strain gage response to the axial load from this test, in units of μV/V/kip, and the radial load sensitivity to range of the strain gage response to be used in the upcoming dynamometer test, in units of kip/V/V).

Table 3. Upwind Bearing Calibration Coefficients

	A		B	
Circumferential Position	**Range Sensitivity to Axial Load (μV/V/kip)**	**Radial Load Sensitivity to Range (kip/V/V)**	**Range Sensitivity to Axial Load (μV/V/kip)**	**Radial Load Sensitivity to Range (kip/V/V)**
0°	10.61	2.70×10^4	7.14	4.02×10^4
90°	8.95	3.20×10^4	9.02	3.18×10^4
180°	10.89	2.63×10^4	7.44	3.85×10^4
270°	10.10	2.84×10^4	5.95	4.82×10^4

Table 4. Downwind Bearing Calibration Coefficients

	C		D	
Circumferential Position	**Range Sensitivity to Axial Load (μV/V/kip)**	**Radial Load Sensitivity to Range (kip/V/V)**	**Range Sensitivity to Axial Load (μV/V/kip)**	**Radial Load Sensitivity to Range (kip/V/V)**
0°	7.60	3.77×10^4	10.84	2.65×10^4
90°	7.14	4.02×10^4	10.81	2.65×10^4
180°	8.43	3.40×10^4	12.08	2.37×10^4
270°	9.88	2.90×10^4	10.96	2.62×10^4

6 Conclusions

An instrumentation package was designed, installed, and calibrated for the tapered roller bearing pair supporting the GRC gearbox HSS assembly. The instrumentation consists of eight strain gage pairs and one RTD installed in axial grooves machined in the outer ring of each bearing. The gages are installed at two axial locations in each of the four equally spaced axial grooves. The gages are wired in a Poisson half-bridge configuration and measure the strain response when a roller passes underneath them, while the RTD simply measures the temperature of the outer ring.

The strain gages underwent calibration testing from May 22–24, 2013, in a 110-kip load frame located at the National Wind Technology Center. The load frame applied up to 50 kip of axial load to the bearing, which was housed in a steel collar representative of the GRC gearbox housing. The maximum applied axial load corresponds to a worst-case radial condition for the bearing in operation in the gearbox. At each load condition, the inner ring of the bearing was rotated 180° manually, resulting in up to four rollers passing underneath each axial groove, and the resulting strain response was measured. In addition, the sensitivity of the strain response to temperature was also measured.

The strain gage response during the bearing rotation was then post-processed to extract the mean and range. A linear regression analysis was used to correlate each measured output with the applied load. It was found that:

- The mean of the strain gage response exhibited a bilinear correlation with applied axial load, with an inflection point of approximately 25 kip. Above this point, the mean was less sensitive to increases in applied load. It is hypothesized this inflection point corresponds to the point at which the diametrical clearance between the outer ring and restraining steel collar was filled. Below this point, the system stiffness is composed of the outer ring alone, and above this point the system stiffness is composed of the outer ring and steel collar.

- The range of the strain gage response exhibited a linear correlation with applied axial load. That is, its response is governed by the local stiffness of the groove in the outer ring, and it is insensitive to the diametrical clearance between the outer ring and steel collar.

- The range of the strain gage response calibration factors varied from 8% to 22% around the circumference of the bearing. Because of the relative size of the strain gage within the groove and subsequent challenge of locating the strain gage pair in the exact center of the groove, it was considered important to calibrate each gage pair individually for both bearings.

- The absolute strain magnitudes (over 450 με) and the strain range (over 200 με) are well within the strain gage pair measurement accuracy. Finite element modeling of the groove geometry under expected operating conditions was valuable in determining the axial groove dimensions to yield these measureable strain values.

- The measured strain gage response was insensitive to temperature. Strain response values changed less than 1% over the range of 24°C to 45°C. This measured strain would only affect test results if the mean strain was used as the metric to determine the applied load. The strain range, which is to be measured over a very short time duration (on the order of seconds), would be unaffected by longer-term changes in temperature.

- In the course of running the tests, the proportional and integral gain factors of the MTS controller for the load frame required adjustment in order to maintain consistent values of applied load while rotating the bearing by hand. It is suspected that because the bearing and load fixture are very stiff systems with very little compliance, small changes in displacement or force while rotating the bearing resulted in the controller applying large loads to compensate. If the test were to be run again, a rubber mat would be added between either the collar and baseplate, or the baseplate and load frame itself. Such a rubber mat would add some compliance and reduce the amount of controller tuning required to maintain consistent applied loads.

7 References

1. Link, H.; LaCava, W.; van Dam, J.; McNiff, B.; Sheng, S.; Wallen, R.; McDade, M.; Lambert, S.; Butterfield, S.; Oyague, F. *Gearbox Reliability Collaborative Project Report: Findings from Phase 1 and Phase 2 Testing.* NREL/TP-5000-51885. Golden, CO: National Renewable Energy Laboratory, 2011.

2. van Dam, J. *Gearbox Reliability Collaborative Bearing Calibration*. NREL/TP-5000-47852. Golden, CO: National Renewable Energy Laboratory, 2011.

3. Sheng, S. "Report on Wind Turbine Subsystem Reliability—A Survey of Various Databases." NREL/PR-5000-59111. Golden, CO: National Renewable Energy Laboratory, 2013.

4. Link, H.; Keller, J.; Guo, Y.; McNiff, B. *Gearbox Reliability Collaborative Phase 3 Gearbox 2 Test Plan*, NREL/TP-5000-58190. Golden, CO: National Renewable Energy Laboratory, 2013.

5. SKF Group. Specification SKF 32222 J2: Tapered roller bearings, single row. http://www.skf.com/group/products/bearings-units-housings/roller-bearings/tapered-roller-bearings/single-row/index.html?prodid=1310002222&nfp=NFP-1310002222#.

6. Austin, J.L. *A Multi-Component Analysis of a Wind Turbine Gearbox using a High Fidelity Finite Element Model*, M.S. Thesis, The Ohio State University, 2013.

7. Jenks, M. *Safe Operating Procedure for Conducting Structural Tests at the NREL NWTC*. SOP-0515. Golden, CO: National Renewable Energy Laboratory, 2013.